# Unsteady Simulations of the Flow in a Swirl Generator, Using OpenFOAM

**Olivier Petit[1], Alin I. Bosioc[2], Håkan Nilsson[1], Sebastian Muntean[3], Romeo F.Susan-Resiga[2]**

[1]Division of Fluid Mechanics, Chalmers University of Technology
Hörsalsvägen 7A, SE-41296 Göteborg, Sweden
olivierp@chalmers.se, hani@chalmers.se
[2]Department of Hydraulic Machinery, "Politehnica" University of Timisoara
Bv. Mihai Viteazu 1, RO 300222, Timisoara, Romania
alin@mh.mec.upt.ro, resiga@mh.mec.upt.ro
[3] Centre of Advanced Research in Engineering Sciences, Romanian Academy – Timişoara Branch
Bv. Mihai Viteazu 24, RO-300223, Timişoara, Romania seby@acad-tim.tm.edu.ro

## Abstract

This work presents numerical results, using OpenFOAM, of the flow in the swirl flow generator test rig developed at Politehnica University of Timisoara, Romania. The work shows results computed by solving the unsteady Reynolds Averaged Navier Stokes equations. The unsteady method couples the rotating and stationary parts using a sliding grid interface based on a GGI formulation. Turbulence is modeled using the standard k-ε model, and block structured wall function ICEM-Hexa meshes are used. The numerical results are validated against experimental LDV results, and against design velocity profiles. The investigation shows that OpenFOAM gives results that are comparable to the experimental and design profiles. The unsteady pressure fluctuations at four different positions in the draft tube is recorded. A Fourier analysis of the numerical results is compared whit that of the experimental values. The amplitude and frequency predicted by the numerical simulation are comparable to those given by the experimental results, though slightly over estimated.

**Keywords**: Swirl generator, OpenFOAM, CFD, Validation, Runner, Draft tube, Rotor-Stator Interaction.

## 1. Introduction

Nowadays, due to the variable demand of the energy market and new intermittent energy sources, a new parameter is often important for water power: flexibility. Water turbines now operate over an extended range of regimes that can be quite far from the best efficiency point. The runner is designed so that the swirl generated by the guide vanes is more or less neutralized by the runner at the best efficiency point. However, at part load operation (away from the efficiency point), a strong swirling flow exits the runner. This is called a vortex rope. This phenomenon leads to large periodic pressure fluctuations that increase the risk of fatigue.

The importance of predicting such phenomena has lead to many studies. One of those is the Flow Investigation in Draft Tubes (FLINDT) research project [1]. The main objective of the FLINDT project was to investigate such phenomena and to provide an extensive database for a range of different operating points. Such experimental projects are usually complex and measurements are performed on reduced scale models. The team at the Politehnica University of Timisoara (UPT), National Centre for Engineering Systems with Complex Fluids (NCESCF) has developed such a simplified swirl generator to further study the precessing vortex rope [2]. The swirl generator was designed to give a swirl profile similar to that in the FLINDT project. The test rig was developed and manufactured in order to provide a good visualization of the phenomenon, as well as to investigate the velocity field of the swirling flow [3, 4]. The stay vanes and runner blades were designed using the inverse design methodology [15] in order to create a precessing vortex rope [5]. One of the purposes of this test rig is to investigate the viability of reducing pressure fluctuation of a precessing vortex rope by axial jet control in the discharge cone. This novel technique was introduced by Susan-Resiga et al. [6] to control the draft tube instability at partial discharge. Measurements on the test rig showed that a 10% jet discharge gives a maximum pressure recovery and creates no pressure fluctuations [7, 17]. This conclusion was asserted by 3D unsteady numerical investigation using Fluent of the swirling flow using jet control [8]. It is nonetheless not acceptable to bypass the runner with such a large fraction of the turbine

This manuscript was presented at the 25th IAHR Symposium on Hydraulic Machinery and Systems, September 20-24, 2010, Politehnica University of Timisoara, Romania .

discharge. However, Susan-Resiga et al. [9, 16] have also developed a flow feedback approach for supplying the jet without any additional energy.

The simple geometry of the test rig, as well as the quality of the measurements performed by Bosioc et al. [10] makes this a very good case study for turbomachinery applications in OpenFOAM. OpenFOAM is an object oriented OpenSource library written in C++. With regards to basic features, such as turbulence models and discretization schemes, OpenFOAM is a competitive and high quality tool that is constantly evolving. Preliminary simulations were realized on the conical diffuser of the test rig [11], which showed that OpenFOAM gives as accurate results as commercial software.

The community driven OpenFOAM Turbomachinery Working Group [12] develops and validates OpenFOAM for turbomachinery applications. The swirling flow generator was chosen as a case study for the 5th OpenFOAM workshop held in Gothenburg, Sweden, and comparison between numerical results and measurements were presented. The goal of the Turbomachinery Working Group is to release this case study so that anyone who would like to learn OpenFOAM, or become more familiar with turbomachinery features in OpenFOAM, can learn how to set up, compute and analyse such problems.

## 2. Experimental setup

A cross-section of the test rig is presented in Fig.1. The original test case was presented by Bosioc et al. [10] and was developed at Politehnica University of Timisoara. The swirling flow apparatus consists of four leaned strouts, 13 guide vanes, a free runner with 10 blades and a convergent divergent draft tube [3-5]. The guide vanes create a tangential velocity component, while keeping practically a constant pressure. The purpose of the free runner is to re-distribute the total pressure by inducing an excess in the axial velocity near the shroud and a corresponding deficit near the hub, like a Francis turbine operation at 70% partial discharge. The runner blades act like a turbine near the hub, and a pump near the shroud. Thus the runner spins freely, without any total torque. The design value for the rotation of the runner is 870 rpm, but stroboscope measurement on the test rig gives a slightly higher rotation, 920 rpm.
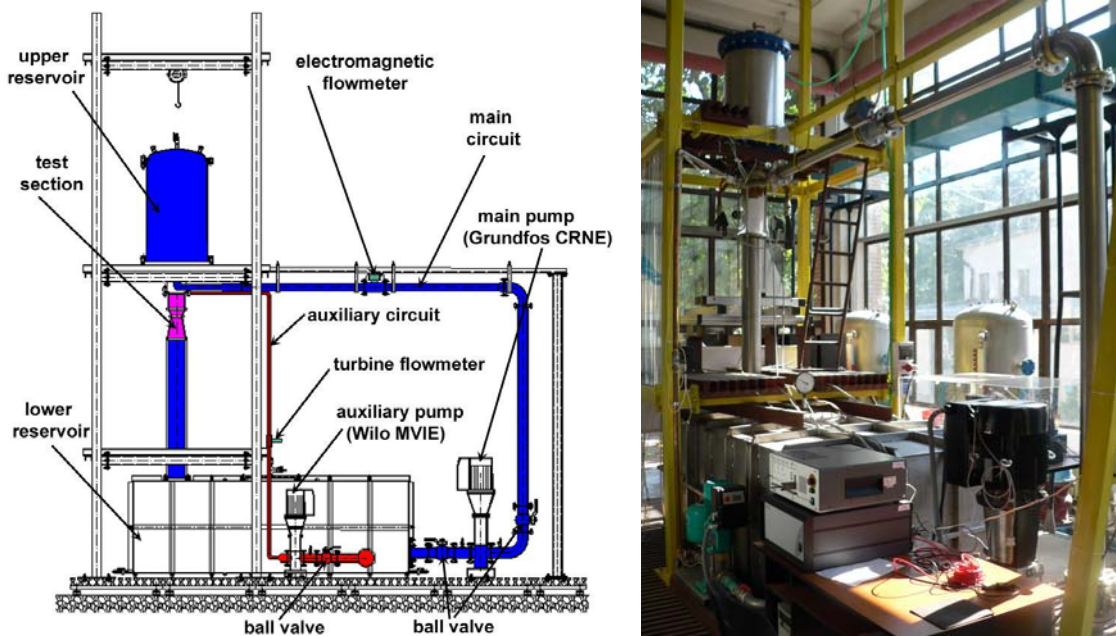


**Fig. 1** Closed loop test rig for experimental investigations of swirling flow installed at Politehnica University of Timisoara.

The test rig consists in a main circuit, used to supply the swirling flow section, and an auxiliary circuit that is used when tests are performed using axial jet control (see Fig.1). The main centrifugal pump that provides the flow has a variable speed delivering up to 35 l/s. The swirling flow test section is made of plexiglass, so that visual observation is possible and to facilitate optical measurements. The measurements were performed at Politehnica University of Timisoara and were first presented by Bosioc et al. [10].

### 2.1 Velocity measurements

The experimental data was measured with the help of two-component Laser-Doppler Velocimetry (LDV). 10 μm aluminum particles were used to reflect the laser beam. The velocity measurements were realized in three different optical windows, the first located in the convergent part of the simplified draft tube, and the other two located in the axi-symmetric diffuser (see Fig. 2). The reference for the survey axis is set at the wall, as shown by the arrows in Fig. 1. On survey axis 0, 31 points were measured, while survey axis 1 contains 113 points, and survey axis 2 contains 141 points. The flow rate was kept at 80% of the maximum power of the pump, that is 30 l/s. The rotational speed of the free runner was 920 rpm. In order to get a time-averaged velocity profile, each point was sampled for a period of 25 seconds (5000 samples). A dimensionless form was used in the analysis of the velocity profiles, normalizing the abscissa by $R_{Throat}$=0.05m, and the velocity profiles by

$$v_{Throat} = \frac{Q}{\pi R_{Throat}^2}, \text{ Q=30 l/s.}$$

For clarity, in the following discussion, the first survey axis is called **W0,** the second survey axis is called **W1** and the third one **W2**.
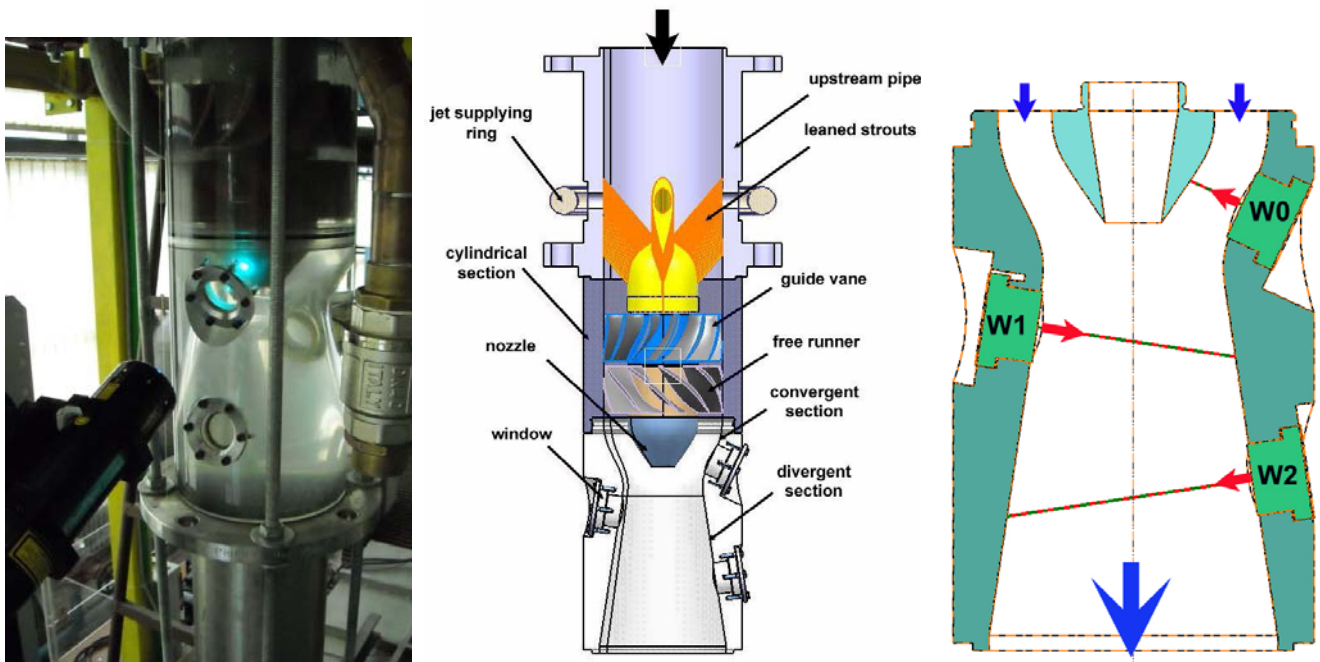
**Fig. 2** Test section for LDV measurements of swirling flow: test section photography (left), cross section of the swirling apparatus in order to measure velocity profiles (centre), survey axes for all three windows (W0, W1 and W2) (right).

## 2.2 Unsteady pressure measurements

The unsteady static pressure is measured at four positions (MG0, MG1, MG2 and MG3) with the help of Cole-Parmer unsteady pressure transducers. The capacitive pressure transducers have an accuracy of 0.13% within a range of ±1 bar relative pressure. When the water is at rest, all pressure transducers are aligned with respect to the static head. For the investigations reported in this paper we are interested in the pressure fluctuations, in order to assess the amplitude and the frequency for the vortex rope from the conical diffuser. Eight of the latter are flush mounted on the cone wall at four levers (see Fig. 3). The sections are located at 0, 50, 100 and 150 mm downstream to the throat. In order to obtain reliable pressure data we measure 100 sets for each discharge value. Each set is acquired using a Lab View program, and corresponds to an acquisition time of 32 seconds at a sampling rate of 256 samples/second, resulting in 8192 samples of unsteady pressure.
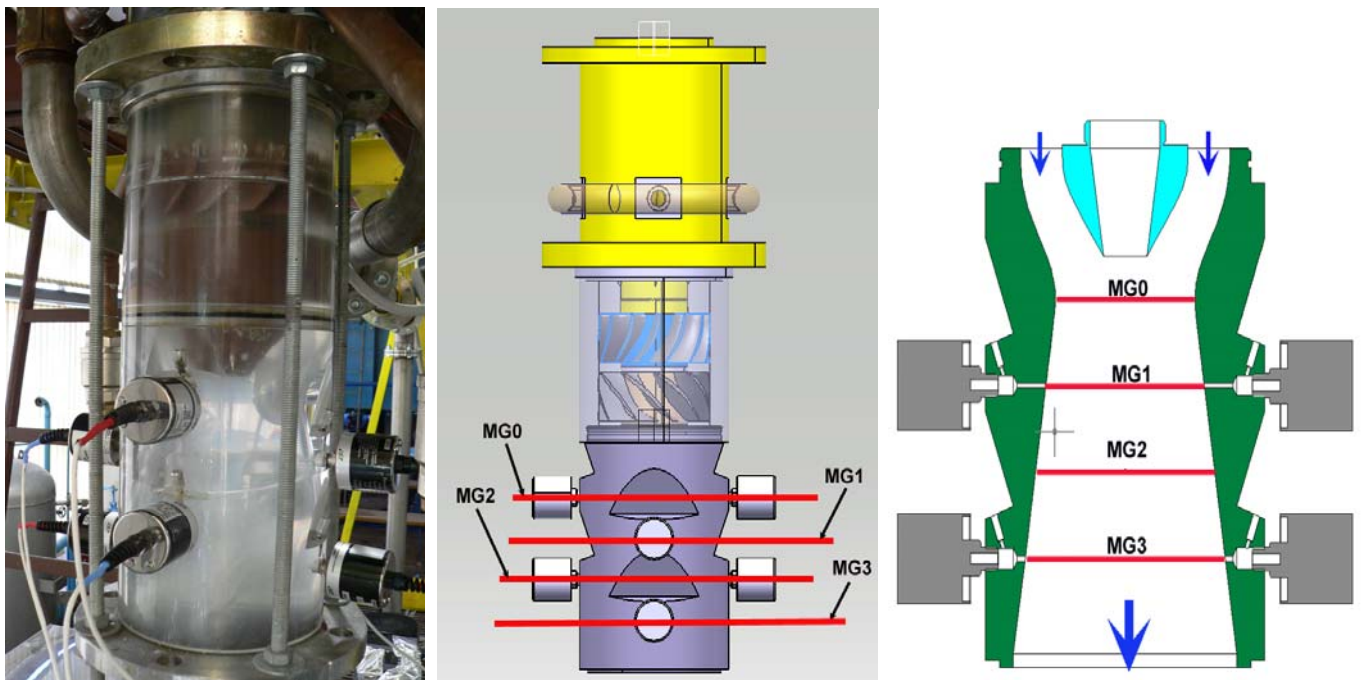


**Fig. 3** Test rig section for unsteady experimental investigations of swirling flow: test section photography (left), unsteady pressure measured on four levels (MG0, MG1, MG2 and MG3) (middle and right).

## 3. Computational domains and OpenFOAM numerical set-up

The computational domain consists of the whole test rig shown in Figs. 2 and 3. The mesh was generated in ICEM-Hexa, and consists of four different parts (see Fig. 4): the leaned strouts, the guide vanes, the free runner and the draft tube. The four different parts are coupled in OpenFOAM using the General Grid Interface (GGI), developed by Beaudoin and Jasak [13]. The

mesh is fully hexahedral, and consists of 2.8 million cells. At the walls, the log-law treatment is applied, and the average y+ values range between 50-200.
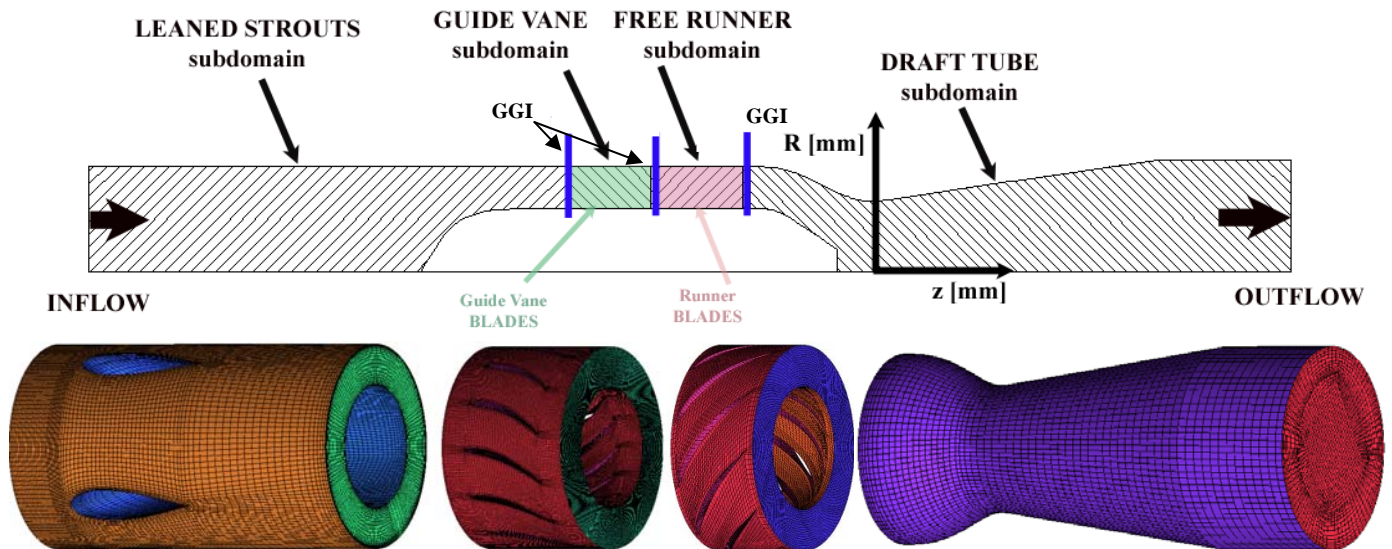


**Fig. 4** Half of meridional cross-section of the swirling flow apparatus (above) and associated computational domains and grids (below).

Two different computational techniques were used to predict the flow in the swirling flow test rig:

- The first method is a steady-state method, solving the steady Reynolds Averaged Navier Stokes equations. Because of the rotor-stator interaction in this case study, a frozen rotor solver is used. It is a steady state formulation where the rotor and stator are fixed with respect to each other, and different reference frames are used in the rotating and stationary parts. Though this method does not predict the flow features behind the runner accurately, it is a fast preliminary method and the general behavior of the flow is predicted. This method is here only used to create an initial solution for the transient method.

- The sliding grid approach is a transient method where the runner mesh actually rotates with respect to the stator mesh. The URANS equations are solved and most of the unsteady flow features are predicted. However, due to the extra dimension added to the resolution (time), the simulation is time and computer resources consuming. The interaction between the rotor and stator is realized with the help of a sliding General Grid Interface [13]. The boundary condition at the inlet is a plug-flow with the nominal discharge 30 l/s. The turbulence kinetic energy is set to 0.1, and the dissipation to 90, so that the turbulence intensity is of the order of 10% and the viscosity ratio $v_T/v$=10. The velocity and turbulence equations use the homogeneous Neumann boundary condition at the outlet. The pressure equation uses a homogeneous Neumann boundary condition at all boundaries, and at the outlet the mean pressure is set to zero. The convection terms are discretized using a second-order linear-upwind scheme, and the time terms are discretized using a second-order backward scheme. The rotation speed of the runner is given by the experimentally measured rotation speed, 920 rpm. The time step used to compute this case is 2.35 $10^{-4}$ s, yielding a maximum Courant number of 5, and a mean Courant number of 0.2. This time step gives an angle of rotation equal to 1.3° per time step.

It was shown in previous studies [14] that the prediction of the flow features by the steady-state method is not accurate enough. Thus the initial condition of the unsteady simulation is generated by the steady simulation, but the present work is focusing only on the unsteady results. A comparison of those results with experimental and design velocity profiles is shown, as well as a Fourier analysis of the pressure fluctuations.

## 4. Comparison of numerical results against experimental and design data

### 4.1 Design and computed velocity profiles

The comparison between the design velocity profiles [5] and the OpenFOAM results is realized at Section 1 (S1) and Section 2 (S2) shown in Fig. 5. Section 1 is downstream the guide vanes, and section 2 is downstream the free runner. The dimensionless velocity profiles are plotted in Fig.6 and 7 against the radius of the different sections, divided by $R_{throat}$. The results computed by OpenFOAM, are time averaged. The two design velocity profiles at sections S1 and S2 were designed to give a specific swirling flow downstream in the draft tube. At section S1, the swirl created by the guide vanes should have a free-vortex configuration, with quasi-constant axial velocity. The numerical results obtained with OpenFOAM are in relatively good agreement with the design profile, see Fig. 6. The axial velocity is in very good agreement in both sections, which shows that the volume flow used in the OpenFOAM simulation is the same as that of the inviscid design theory. However, the numerical simulation over-estimates the tangential velocity at section S2, located below the runner. The design value of the rotation speed of the free runner was 870 rpm. Nevertheless, after the construction of the test rig, the experimentally measured rotation speed of the runner turned to be equal to 920 rpm, slightly higher than the intended design value. The rotation speed in numerical simulation is 920 rpm. This is why the tangential velocity obtained in the simulation is higher than the tangential velocity for the inviscid design. Complementary studies with the help of OpenFOAM [18] has shown that if the rotation speed of the free runner is lowered to the value given by the inviscid design, the tangential velocity obtained with OpenFOAM corresponds to that of the inviscid theory.
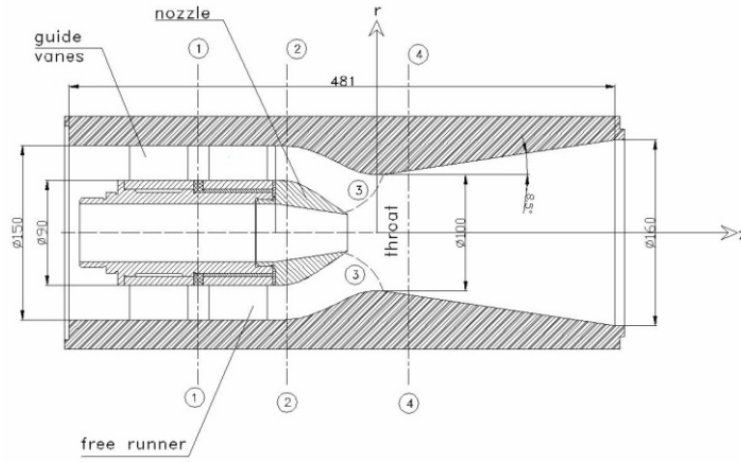
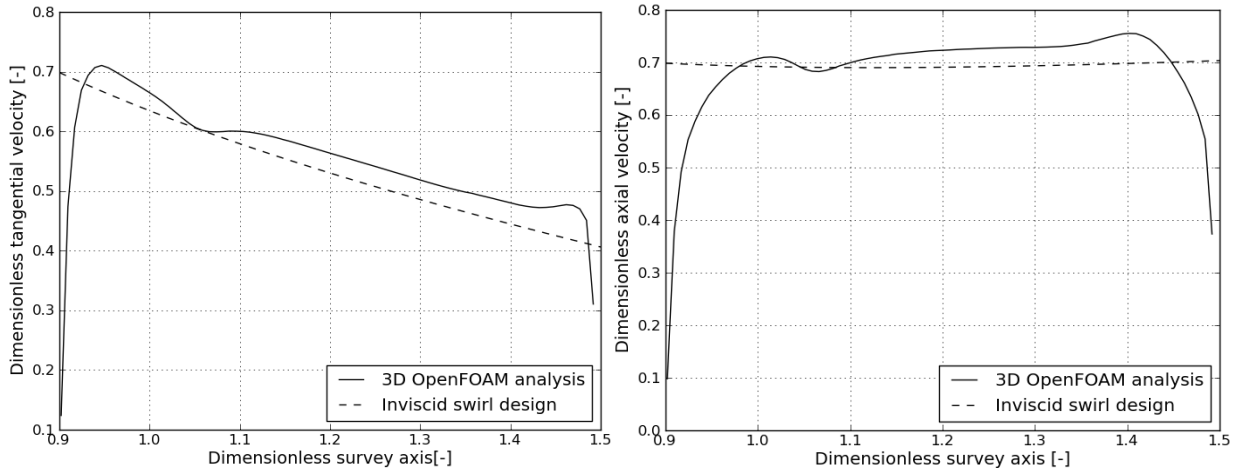**Fig. 5** Cross-section of the swirling flow apparatus and the four survey axes.



**Fig. 6** Tangential (left) and axial (right) velocity profiles at section S1, displaced between guide vanes and free runner (Fig. 5).
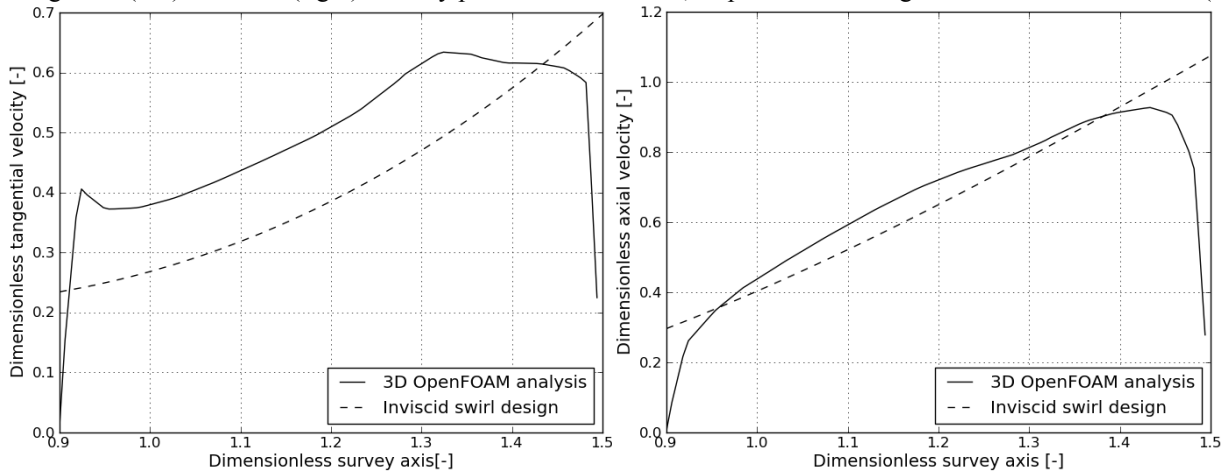


**Fig. 7** Tangential (left) and axial (right) velocity profiles at S2, displaced just downstream to the free runner (Fig. 5).

### 4.2 Experimental and computed velocity profiles in test the section

The comparisons between the velocity profiles numerically predicted with OpenFOAM, and the experimental data are shown in Fig. 8. The computed velocity profiles are time averaged. At section W0, the velocity computed by OpenFOAM shows very good agreement with that of the experiment. However, the computed tangential velocity is a bit under-predicted. The slight underestimation of the tangential has an impact on the meridional velocity at sections W1 and W2. Since the tangential velocity is not as large as it should be, more flow is pushed close to the walls, and less in the centre line. It can be seen that the stagnation region predicted by the measurements is becoming a recirculation region for the computed flow, with a small negative meridional velocity.

As shown in Fig. 8, the wakes of the 10 runner blades can still be seen at window W0, and the region of the precessing vortex rope, with a zero or negative tangential velocity can be seen at window W1 and W2. The unsteady simulation predicts the periodic fluctuations in the draft tube rather well, and a visualization of the computed vortex rope is shown in Fig. 9. Due to the time resolution of the sliding grid model, the visualization of the vortex rope oscillation can be done. Fig. 9 also shows the same vortex rope visualized in the experiments.
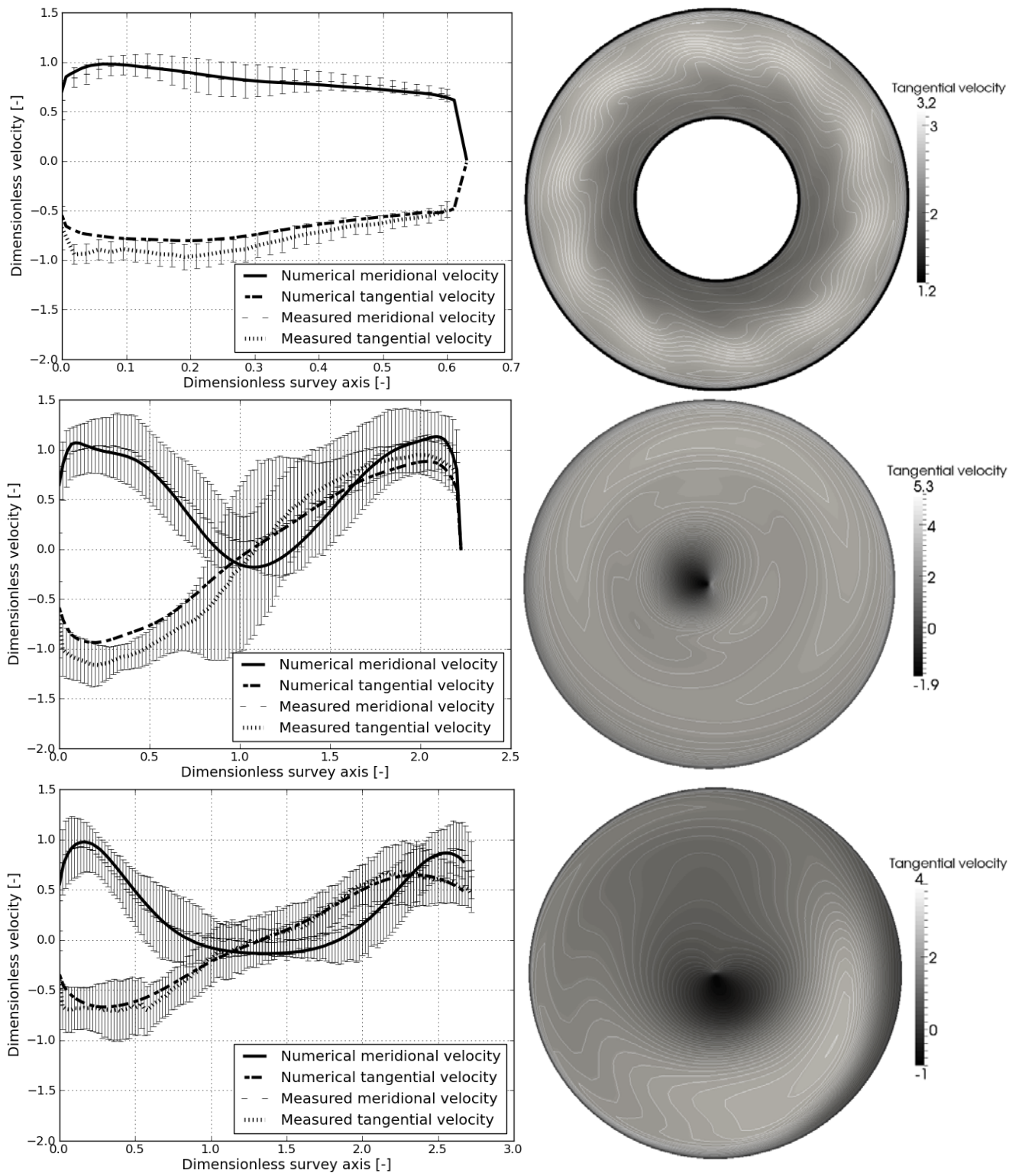
**Fig. 8** Time-averaged velocity profiles (left), and instantaneous tangential velocity (right) at W0, W1, W2 ( top to bottom).
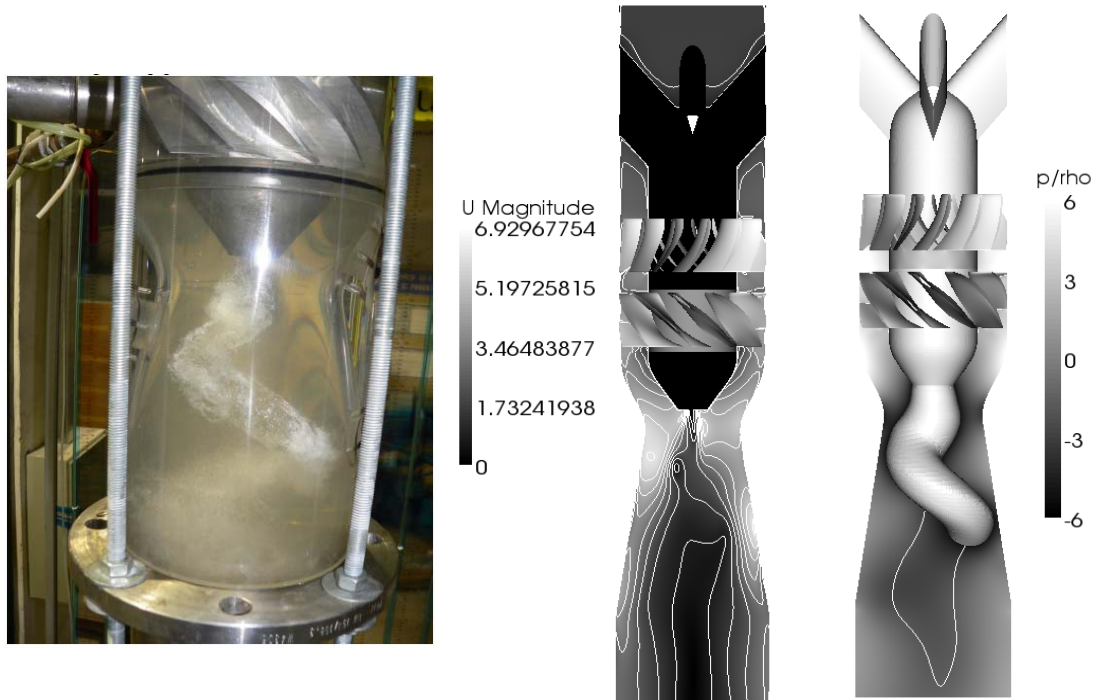
**Fig. 9** The precessing vortex rope visualized in the experimental test section (left), and snap-shots of the velocity (centre) and pressure field (right) predicted by the numerical simulations in OpenFOAM. For the pressure snap-shot, the iso-surface visualizes a surface of constant pressure, while the iso-line shows where the axial velocity is zero.

### 4.3 Fourier analysis of the pressure fluctuations

The recorded pressure fluctuations at the four different draft-tube locations, MG0-MG3 (see Fig. 3), are examined using a Fourier analysis. Let $f$ be a real periodic valued function of time with period T. Suppose we sample $f$ at $N$ equally spaced time interval of length $\Delta$ seconds starting at time $t_0$. That is we have $s_i = f(t_0 + i\Delta)$, $i = 0,1,...,N-1$. In particular, it assumes that $f(t_0) = f(t_0 + N\Delta)$. Hence, the period is assumed to be $T = N\Delta$. The interpolating trigonometric polynomial g(t) which approximates the function $f(t)$ can be written as

$$g(t) = A_0 + \sum_{n=1}^{(N-1)/2} A_n \cos[\omega_n(t - t_0)] - \sum_{n=1}^{(N-1)/2} B_n \sin[\omega_n(t - t_0)]$$

with

$$A_0 = \frac{c_0}{N} = \frac{1}{N}\sum_{n=0}^{N-1} s_n, \quad A_n = \frac{2c_{2n}}{N}, \quad B_n = \frac{2c_{2n+1}}{N}, \text{ and } \quad \omega_n = \frac{2\pi(n+1)}{N\Delta} = \frac{2\pi(n+1)}{T}$$

$A_0$ is the average value of the samples, while $A_n$ and $B_n$ are respectively the cosine and sine modes amplitudes for the angular frequency $\omega_n$.

The FFTRF subroutine from International Math and Statistics Libraries (IMSL) is used to compute the discrete Fourier transform and the reconstruction signal. The numerical unsteady pressure recorded in all monitors (MG0-MG3) as well as the reconstruction signals are plotted, and the corresponding frequency spectra are plotted in Fig. 10.

As shown in Fig. 10, the simulation performed in OpenFOAM over-estimates the amplitude of the vortex rope at all the four different probes positions. At MG1, MG2 and MG3, the numerical prediction of vortex rope amplitude is largely over-estimated, relative to the experimental data. This means that the vortex rope is well developed and more compact for a longer distance in the numerical computation than in the experimental investigation. This conclusion asserts the previous comparisons between numerical and experimental investigations of the vortex rope [11]. The numerical computation using the k-ε turbulence model over-estimates the amplitude of the vortex rope, predict a more compact vortex rope than the experimental investigation, and fails to predict accurately the dispersion of the vortex rope.

However, what is more unexpected is the shift in the frequency of the vortex rope between the experimental value and the numerical one. The frequency of the vortex rope predicted by the simulation is about 18.5 Hz, while it was measured around 15.5 Hz with the pressure transducers (Fig. 10). The computed results show as well a harmonic around 15.3 Hz, which corresponds to the frequency of the runner rotating.

Though numerical results overestimates the amplitude of the vortex rope, it is very interesting to notice that the numerical simulation succeeds in successfully computing an oscillation in the axial direction of the vortex rope. This oscillation can be seen in Fig. 10 on the right, at all the different positions, and the frequency of this oscillation is around 3 Hz (see Fig. 10, left). This oscillation of the vortex rope can be seen as well in the latest experimental investigation [16].
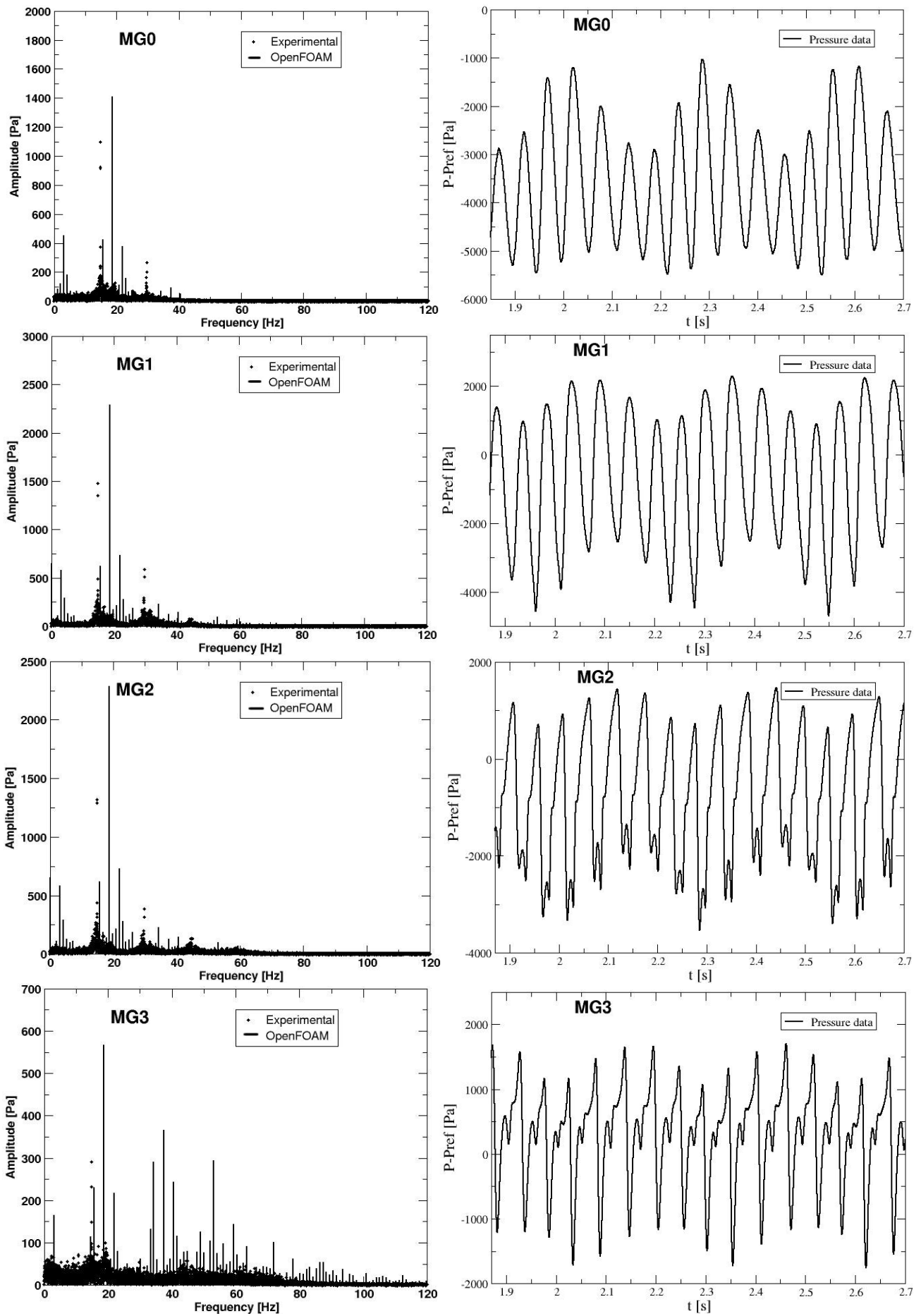
**Fig. 10** Fourier analysis (left ) of the numerical pressure data (right) at the four positions MG0-MG3 (from top to down)

### 4.4 Importance of the time step in transient rotor-stator simulations

As the numerical simulation solves the Unsteady Reynolds Averaged Navier-Stokes equation, the time dependency is taken into account. Fig. 11 presents a comparison between the previously described simulation, Case 1, with a time step of $2,35 \cdot 10^{-4}$ s, yielding a maximum Courant number of 5 and an angle of 1.3° per time step, and a more detailed simulation, Case 2, with a time step of $4,76 \cdot 10^{-5}$ s, yielding a maximum Courant number of 1, and an angle of 0.25° per time step. Both simulations start from the same initial conditions from the same settings as Case 1. Thus the Case 2 results experience an initial transient, and the flow is not to be considered developed. Case 2 predicts the wakes of the runner blades at MG0, while Case 1 doesn't (Fig. 11). Moreover, one can see that the prediction of the vortex rope frequency in Case 2 seems to develop to a lower one than in Case 1. However, the computation time is increase by a factor of 4,5 for Case 2, so it is necessary to achieve a balance between the computational time and the accuracy of the results.
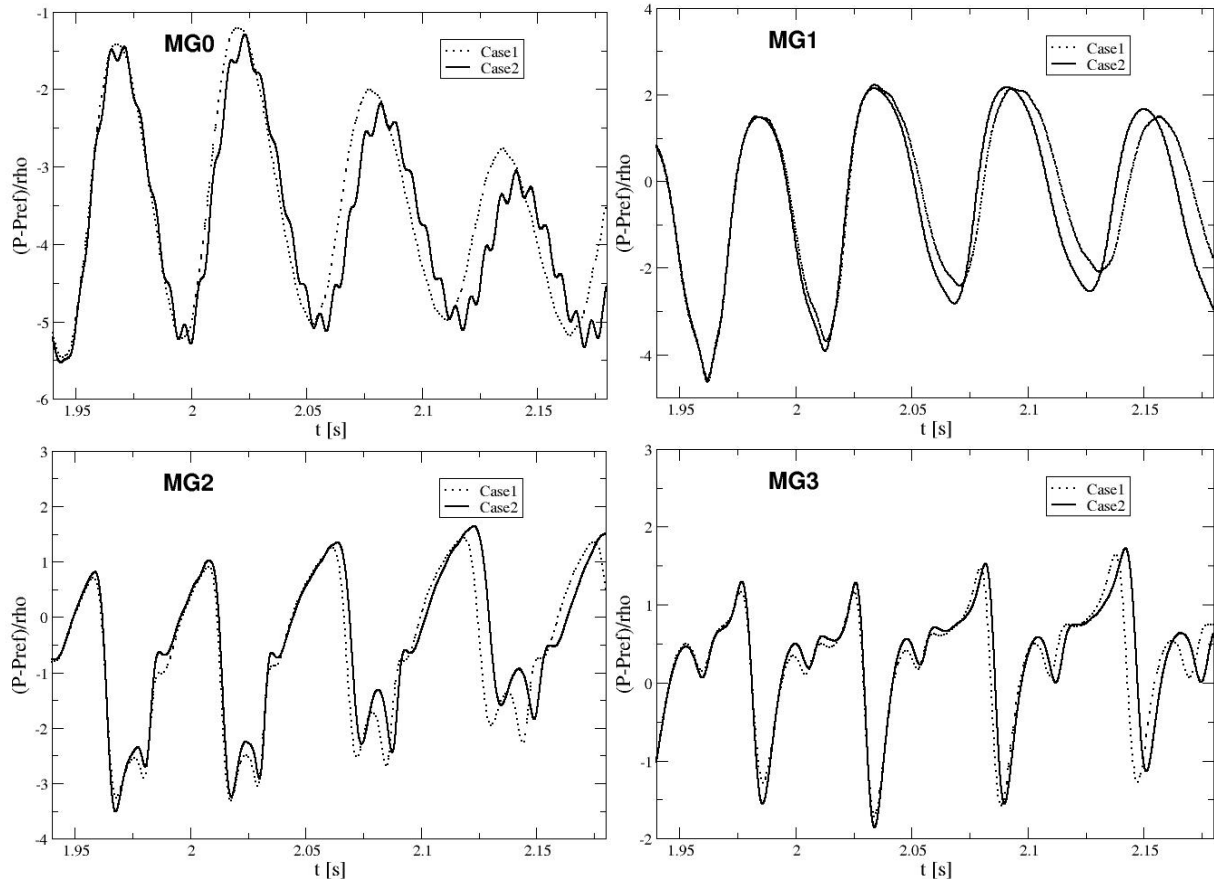


**Fig. 11** Comparison between Case 1(Courant number of 5), and Case 2 (Courant number of 1) for the four pressure transducers positions MG0-MG3.

## 5. Conclusion

We present in this paper the unsteady three-dimensional numerical investigations of the swirling flow with helical vortex breakdown in a conical diffuser, quite similar to the flow encountered in Francis turbines draft tube cone when operating at partial discharge. The three-dimensional computational domain corresponds to the test section installed on test rig at Politehnica University of Timisoara. The full three-dimensional flow is computed with the help of a transient method, using the standard k-ε model available in OpenFOAM.

First, the velocity profiles computed with OpenFOAM are in good agreement with the design profiles upstream and downstream to the free runner. The axial velocity is in very good agreement in both sections, which shows that the discharge imposed in the OpenFOAM simulation is the same as that of the inviscid design theory. As expected, the numerical simulation over-estimates the tangential velocity at section S2, located downstream the runner. The discrepancy corresponds to the difference between design runner speed 870 rpm and value measured on the test rig 920 rpm.

Second, the time average computed velocity profiles are validated with experimental data along to the three sections W0 (situated in the convergent part), W1 and W2 (both displaced in the conical section). The velocity computed by OpenFOAM shows good agreement with experiment data.

Finally, the unsteady pressure computed numerically with OpenFOAM is compared with experimental data. The simulation performed in OpenFOAM overestimates the amplitude of the vortex rope at all the four different probes positions. The fundamental frequency of the vortex rope is rather well predicted, but by reducing the time step of the transient computation, a more accurate prediction of the frequency and amplitude of the vortex rope may be achieved.

# Acknowledgements

# References

[1] Avellan, F., 2000, "Flow Investigation in a Francis Draft Tube: The FLINDT Project," in Proceedings of the 20th IAHR Symposium on Hydraulic Machinery and Systems, Charlotte, USA, Paper DES-11.

[2] Susan-Resiga, R., Muntean, S., Bosioc, A., Stuparu, A., Milos, T., Baya, A., Bernad, S., and Anton, L.E., 2007, "Swirling Flow Apparatus and Test Rig for Flow Control in Hydraulic Turbines Discharge Cone," in Proceedings 2nd IAHR International Meetings of the Workgroup in Cavitation and Dynamic Problems in Hydraulic Machinery and Systems, Scientific Bulletin of the Politehnica University of Timisoara, Transcations on Mechanics, Vol. 52(66), Fasc.6, pp. 203-216.

[3] Susan-Resiga, R., Muntean, S., Tanasa, C., and Bosioc, A., 2008, "Hydrodynamic Design and Analysis of a Swirling Flow Generator," in Proceedings of the 4th German – Romanian Workshop on Turbomachinery Hydrodynamics (GRoWTH), June 12-15, 2008, Stuttgart, Germany.

[4] Bosioc, A., Susan-Resiga, R., and Muntean, S., 2008, "Design and Manufacturing of a Convergent-Divergent Test Section for Swirling Flow Apparatus," in Proceedings of the 4th German – Romanian Workshop on Turbomachinery Hydrodynamics (GRoWTH), June 12-15, 2008, Stuttgart, Germany.

[5] Susan-Resiga, R., Muntean, S., and Bosioc, A., 2008, "Blade Design for Swirling Flow Generator," in Proceedings of the 4th German – Romanian Workshop on Turbomachinery Hydrodynamics (GRoWTH), June 12-15, 2008, Stuttgart, Germany.

[6] Susan-Resiga, R., Vu, T.C., Muntean, S., Ciocan, G.D., and Nennemann, B., 2006, "Jet Control of the Draft Tube Vortex Rope in Francis Turbines at Partial Discharge," in Proceedings of the 23rd IAHR Symposium on Hydraulic Machinery and Systems, Yokohama, Japan, Paper F192.

[7] Muntean, S., Susan-Resiga, R., Bosioc, A., Stuparu, A., Baya, A., Anton, L.E., 2008, "Mitigation of Pressure Fluctuation in a Conical Diffuser with Precessing Vortex Rope Using Axial Jet Control Method," in Proceedings of the 24th IAHR Symposium on Hydraulic Machinery and Systems, Foz do Iguassu, Brazil.

[8] Muntean, S., Susan-Resiga, R., and Bosioc, A., 2009, "Numerical Investigation of the Jet Control Method for Swirling Flow with Precessing Vortex Rope," in Proceedings of the 3rd IAHR International Meeting of the Workgroup on Cavitation and Dynamic Problems in Hydraulic Machinery and Systems, Vol. I, Brno, Czech Republic. Paper B2 pp. 65-74

[9] Susan-Resiga, R., and Muntean, S., 2008, "Decelerated Swirling Flow Control in the Discharge Cone of Francise Turbines," in Proceedings of the 4th International Symposium on Fluid Machinery and Fluid Engineering, Beijing, China. Paper IL-18.

[10] Bosioc, A., Susan-Resiga, R., and Muntean, S., 2009, "2D LDV Measurements od Swirling Slow in a Simplified Draft Tube," in Proceedings of the CMFF09, Vol. II, Budapest, Hungary. pp. 833-838

[11] Muntean, S., Nilsson, H., and Susan-Resiga, R., 2009, "3D Numerical Analysis of the Unsteady Turbulent Swirling Flow in a Conical Diffuser Using Fluent and OpenFOAM," in Proceedings of the 3rd IAHR International Meeting of the Workgroup on Cavitation and Dynamic Problem in Hydraulic Machinery and Systems, Brno, Czech Republic.

[12] Nilsson, H., Page, M., Beaudoin, M. and Jasak H., 2008, "The OpenFOAM Turbomachinery Working Group, and Conclusions from the Turbomachinery Session of the Third OpenFOAM Workshop," in Proceedings of the 24th IAHR Symposium on Hydraulic Machinery and Systems, Foz do Iguassu, Brazil.

[13] Beaudoin, M., and Jasak, H., 2008, "Development of a Generalized Grid Interface for Turbomachinery simulations with OpendFOAM," in Proceedings of the OpenSource CFD International Conference, Berlin, Germany.

[14] Petit, O., Nilson, H., Page, M. and Beaudoin, M., 2009, "The ERCOFTAC Centrifugal Pump OpenFOAM Case-Study," in Proceedings of the 3rd IAHR International Meeting of the Workgroup on Cavitation and Dynamic Problem in Hydraulic Machinery and Systems, Brno, Czech Republic.

[15] Zangeneh, M, 1991, "A Compressible Three-Dimensional Design Method for Radial and Mixed Flow Turbomachinery Blades," International Journal for Numerical Methods in Fluids, 13, pp. 599-624.

[16] Tanasa C., Susan-Resiga R., Bosioc A. and Muntean S., 2010, "Mitigation of Pressure Fluctuations in the Discharge Cone of Hydraulic Turbines Using Flow-Feedback," in Proceedings of the 25th IAHR Symposium on Hydraulic Machinery and Systems, Timisoara, Romania (IOP Conf. Series: Earth and Environmental Science 12 012067 doi:10.1088/1755-1315/12/1/012067.

[17] Bosioc. A., Tanasa C., Muntean S. and Susan-Resiga F., 2010, "Unsteady Pressure Measurements and Numerical investigation of the Jet Control Method in a Conical Diffuser with Swirling Flow," in Proceedings of the 25th IAHR Symposium on Hydraulic Machinery and Systems, Timisoara, Romania (IOP Conf. Series: Earth and Environmental Science 12 012017 doi:10.1088/1755-1315/12/1/012017.

[18] Bergman O., 2010, "Numerical Investigation of the Flow in a Swirl Generator, Using OpenFOAM," Master's Thesis in Fluid Mechanics, Chalmers University of Technology, Division of Fluid Mechanics.